Electron-nuclear double resonance of Ga in Mn-doped GaP

P. van Engelen
Philips Research Laboratories, Eindhoven, The Netherlands
(Received 5 February 1979; revised manuscript received 29 January 1980)

The hyperfine interactions of the first shell of Ga neighbors around Mn^{2+} on a Ga site in GaP are determined at 4.2 K by means of electron-nuclear double resonance (ENDOR) techniques. The spectrum could be described by use of the ENDOR spin Hamiltonian $\mathcal{H}=\vec{I}\cdot\vec{A}\cdot\vec{S}+Q'[I_{x_q}^2-\frac{1}{3}I(I+1)+\frac{1}{3}\eta(I_{y_q}^2-I_{z_q}^2)]-g_N\beta_N\vec{H}\cdot\vec{I}$. The parameters of ^{71}Ga are: $A_{x_hx_h}/h=+16.665\pm0.004$ MHz, $A_{y_hy_h}/h=+14.186\pm0.010$ MHz, $A_{z_hz_h}/h=+13.848\pm0.008$ MHz, $Q'/h=-1.493\pm0.005$ MHz, $\eta=0.20\pm0.02$, and $g_N\beta_N/h=+1.298\pm0.003$ kHz/G. The x_h, y_h, and z_h axes are the principal axes of $\vec{A}$. The z_h and z_q axes coincide, and are along $[\bar{1}10]$ for a Mn-Ga pair with axis along [110]. The angles between the pair axis and the x_h and x_q axes are $32.2\pm0.2°$ and $42.6\pm0.3°$, respectively. The results for ^{69}Ga are found to scale with those for ^{71}Ga according to the ratios of the nuclear spins and the quadrupole moments. An attempt is made to interpret the data in terms of electron transfer and point-charge contributions.

I. INTRODUCTION

Investigations of the hyperfine interaction (hfi) between a paramagnetic ion and nearest cation neighbors are of interest for the understanding of transfer mechanisms.[1] This particular type of hfi, called cation-cation hfi, has already been studied in detail for the systems $LaAlO_3$:Fe^{3+} and Cr^{3+}.[2] For more covalent systems, such as the II-VI (Ref. 3) and III-V compounds, a detailed study is however not available. Some information has been obtained for CdTe:Cr^{+}.[4] For Fe^{3+} in GaP and GaAs,[5] where Fe^{3+} is most likely at a Ga site, ENDOR (electron-nuclear double resonance) transitions due to nearest cation neighbors have not been observed.

This paper presents results of an ENDOR investigation of the cubic Mn^{2+} center in GaP, with emphasis on the magnetic hfi and the electric quadrupole interaction (QI) of nearest ^{69}Ga and ^{71}Ga neighbors. A simple model based on electron transfer and point-charge contributions, enables us to explain the magnetic hfi and roughly half of the QI. A preliminary account of this work has been presented elsewhere.[6]

II. NATURE OF Mn^{2+} CENTER

GaP has the zinc-blende structure. Mn can substitute at a Ga site. A unit cell of GaP with the Mn impurity at the central Ga site is shown in Fig. 1. The first- and second-nearest neighbors of Mn consist of

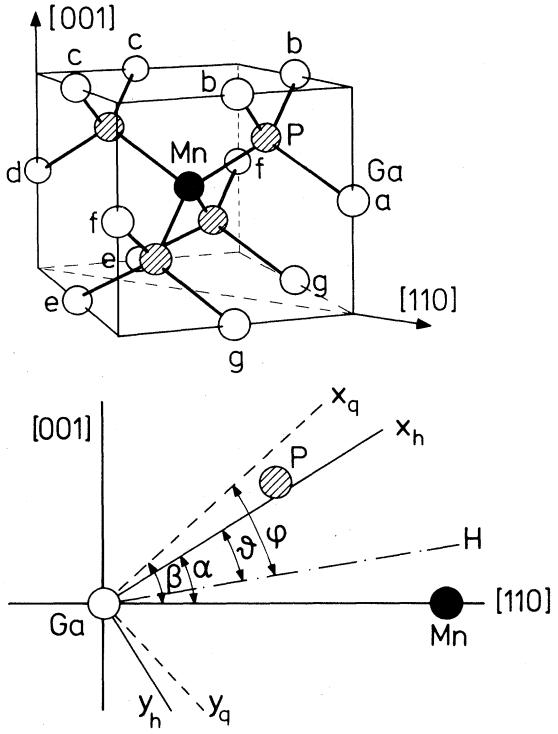

FIG. 1. Upper part: unit cell of GaP, showing the substituted Mn surrounded by 4 nearest P and 12 nearest Ga neighbors (labeled *a* to *g*). Lower part: position of the principal axes of the Ga magnetic hfi tensor (x_h,y_h,z_h) and QI tensor (x_q,y_q,z_q) of a Mn-Ga nearest neighbor pair. The *x* axes are those with the largest absolute value of the tensor elements. The angle $\alpha(\beta)$ measured from x_h (x_q) to [110] is taken to be positive if the *x* axis lies in the same quadrant as the P atom. Angles ϑ and φ are those between $\vec{H}$ and the x_h and x_q principal axes, respectively.

4 and 12 ions, respectively.

In the trivalent state Mn is neutral with respect to the lattice, and is an acceptor[7] with an energy level at 0.40–0.45 eV from the valence band.[8] The divalent state is the compensated acceptor state,[9] made possible by electron transfer from donors present in the crystal. The difference of the concentrations of Mn and donors determines the conductivity (p or n type). In addition, with an excess of donors all Mn ions will be in the divalent state. If the donor is situated at a large distance from the Mn^{2+} ion, the latter is essentially in a cubic environment. A donor, e.g., S, at one of the first P neighbor sites results in a Mn^{2+} center with trigonal symmetry.[10] The EPR spectrum of our samples, doped with Mn and S, therefore is a superposition of at least two types of spectra, namely, a spectrum due to cubic Mn^{2+} and spectra due to four equivalent Mn^{2+}-S pair centers with trigonal symmetry around $\langle 111\rangle$. These spectra range from approximately 1900 to 4900 G at 9500 MHz. The cubic Mn^{2+} center yields six broad lines (25–30 G peak to peak) with unresolved cubic field splitting. The EPR parameters of the cubic[7,11] and the trigonal[10] center have earlier been reported. More accurate ^{55}Mn hfi and cubic field splitting parameters of the cubic center have earlier been determined by ENDOR measurements on ^{55}Mn.[12]

III. Ga ENDOR MEASUREMENTS

A. Spin Hamiltonian and energy levels

Let us consider the interaction between Mn^{2+} and the shell of 12 nearest Ga neighbors. The symmetry of each Mn-Ga pair corresponds to C_s about the Ga ion, e.g., a pair lying in the $(\bar{1}10)$ plane has only reflection symmetry in that plane, and the $[\bar{1}10]$ direction therefore is a principal axis of the Ga hfi tensors. In Fig. 1 the set of principal axes of the magnetic hfi tensor (x_h,y_h,z_h) and of the QI tensor (x_q,y_q,z_q) are drawn for such a pair. The principal x (and y) axes do not necessarily coincide because they do not arise from the same interactions. We take x_h and x_q to be the axes with the largest absolute value of the tensor elements. The positions of x_h and x_q relative to [110] are defined by the angles α and β (with absolute values smaller than $\frac{1}{2}\pi$). Each of the angles is taken to be positive if the principal x axis lies in the same quadrant as the P atom of the Mn-P-Ga$_i$ configuration in Fig. 1.

Experimentally we find that the ENDOR transitions are well described by considering single Mn^{2+}-Ga pairs. Splittings of ENDOR transitions arising from indirect nuclear spin-spin interaction[13] between magnetically equivalent Ga nuclei are not observed. The relevant spin Hamiltonian for a pair then is

$$\mathcal{H}=g\beta\vec{H}\cdot\vec{S}+\tfrac{1}{6}a\,[S_\xi^4+S_\eta^4+S_\zeta^4-\tfrac{1}{5}S(S+1)(3S^2+3S-1)]+A_{\mathrm{Mn}}\vec{I}_{\mathrm{Mn}}\cdot\vec{S}-g_{\mathrm{Mn}}\beta_N\vec{H}\cdot\vec{I}_{\mathrm{Mn}}$$
$$+\vec{I}_{\mathrm{Ga}}\cdot\vec{A}_{\mathrm{Ga}}\cdot\vec{S}-g_{\mathrm{Ga}}\beta_N\vec{H}\cdot\vec{I}_{\mathrm{Ga}}+Q'[I^2_{\mathrm{Ga},x_q}-\tfrac{1}{3}I_{\mathrm{Ga}}(I_{\mathrm{Ga}}+1)+\tfrac{1}{3}\eta(I^2_{\mathrm{Ga},y_q}-I^2_{\mathrm{Ga},z_q})]\ . \tag{1}$$

The terms have the usual meaning, ξ, η, and ζ being the cubic axes. Further, $S=\frac{5}{2}$, $I_{\mathrm{Mn}}=\frac{5}{2}$, and $I_{\mathrm{Ga}}=\frac{3}{2}$ both for ^{69}Ga and ^{71}Ga with 60.4 and 39.6% natural abundance, respectively.

The relative magnitudes of the terms of Eq. (1) are such that the energy levels can be calculated by perturbation theory. We will use this for the identification of the ENDOR transitions. The largest term in Eq. (1) is $g\beta\vec{H}\cdot\vec{S}$, so it is convenient to choose $S_z\|\vec{H}$ and to use the zero-order electron-spin states $|M\rangle$. The second and third term mix the $|M\rangle$ states. We will assume for the moment that the mixing is negligible, which has the consequence that the second and third term are of no importance for the Ga ENDOR transitions. Similarly, the fourth term may be omitted. The second largest term is then the isotropic part of the Ga hfi, so we take $I_{\mathrm{Ga},z}\|S_z$ and use the basic states $|M,m_{\mathrm{Ga}}\rangle$. In order to describe the experiments with $\vec{H}$ in the $(\bar{1}10)$ plane, we derived an expression for the Ga ENDOR transitions as a function of the angles ϑ and φ defined in Fig. 1. To second order it reads

$$E_{M,m}-E_{M,m-1}=MA_0-g_N\beta_NH+\tfrac{1}{2}Q'(2m-1)(3\cos^2\varphi-1+\eta\sin^2\varphi)$$
$$-\frac{S(S+1)-M^2}{2g\beta H}A_1A_{z_hz_h}-\frac{M(2m-1)}{4g\beta H}(A_1^2+A^2_{z_hz_h}-2A_2^2)$$
$$+\frac{Q'^2}{8(MA_0-g_N\beta_NH)}[\sin^2\varphi+\tfrac{1}{3}\eta(1+\cos^2\varphi)]^2[2I(I+1)-3(2m^2-2m+1)]$$
$$+\frac{1}{MA_0-g_N\beta_NH}\{\delta^2Q'^2[12m^2-12m+\tfrac{9}{2}-2I(I+1)]+3(2m-1)M\delta Q'A_2+\tfrac{1}{2}M^2A_2^2\}\ . \tag{2}$$

Here $A_0=A_{x_hx_h}\cos^2\vartheta+A_{y_hy_h}\sin^2\vartheta$, $A_1=A_{x_hx_h}\sin^2\vartheta+A_{y_hy_h}\cos^2\vartheta$, $A_2=(A_{y_hy_h}-A_{x_hx_h})\sin\vartheta\cos\vartheta$, and $\delta=-\sin\varphi\cos\varphi(1-\frac{1}{3}\eta)$. Because the Mn nuclear-spin terms are left out, the subscript Ga could be dropped in

Eq. (2). For $\vec{H} \| z_h (= z_q)$ the energy differences are

$$E_{M,m} - E_{M,m-1} = MA_{z_h z_h} - g_N \beta_N H - \tfrac{1}{2} Q'(2m-1)(1+\eta) - \frac{S(S+1)-M^2}{2g\beta H} A_{x_h x_h} A_{y_h y_h} - \frac{M(2m-1)}{4g\beta H}(A^2_{x_h x_h} + A^2_{y_h y_h}) + \frac{Q'^2(1-\frac{1}{3}\eta)}{8(MA_{z_h z_h} - g_N \beta_N H)}[2I(I+1) - 3(2m^2-2m+1)] \quad . \tag{3}$$

It must be noted that the approximation involved in the use of perturbation theory resulting in those terms of Eqs. (2) and (3) with denominator $MA - g_N \beta_N H$, is better for large $|M|$. This is because the ratios of the off-diagonal matrix elements to the energy difference $MA - g_N \beta_N H$ decrease for increasing $|M|$. Further, Eqs. (2) and (3) were derived under the assumption that we are dealing with zero-order electron-spin states $|M\rangle$. As we have seen, however, the second and third term of the spin Hamiltonian, Eq. (1), mix these states. If mixing is allowed for, the cubic crystal field term ($a/h = +30$ MHz) affects the calculated Ga ENDOR frequencies, Eqs. (2) and (3), by at most 1 kHz and can be neglected, whereas the ^{55}Mn hfi ($A/h = -159$ MHz) in general results in shifts of the order of 100 kHz. However, the latter shift vanishes for the states $|M, m_{Mn}\rangle = |+\frac{5}{2}, +\frac{5}{2}\rangle$ and $|-\frac{5}{2}, -\frac{5}{2}\rangle$ because the off-diagonal matrix elements of the ^{55}Mn hfi involving these states are zero. Thus, in order to get a good set of parameters using Eqs. (2) and (3), the Ga ENDOR transitions were measured for the latter states.

B. Experimental

The ENDOR experiments were carried out at 4.2 K with a 3-cm homodyne EPR spectrometer. An rf coil (5–10 turns) was wound around the sample which is placed in the center of a rectangular TE_{102} cavity. The spectra were recorded at fixed magnetic field and frequency modulated (230 Hz) rf field. We used two kinds of samples, namely, solution-grown[10] and LEC (liquid-encapsulated-Czochralski)-grown crystals, both doped with Mn and S. Both the EPR and ENDOR spectra were found to be the same. The samples had typical Mn and S concentrations of 5×10^{18} and 1×10^{19} cm^{-3}, respectively.

C. ENDOR spectrum

The ENDOR spectrum observed can be divided into two main parts. Above 50 MHz ENDOR lines were found that are solely due to ^{55}Mn nuclear-spin flips. Below 50 MHz the spectrum contains as many as 200 lines which are ascribed to neighboring Ga atoms. From the EPR linewidth an upper limit of 50 MHz for the hfi with the P ligands is obtained. Consequently, ENDOR of ^{31}P is to be expected below ~ 150 MHz. We could not find lines attributable to ^{31}P, however.

With $\vec{H}$ set arbitrarily within the EPR spectrum, we found Ga ENDOR transitions for all $|M\rangle$ states. The linewidth of the ENDOR lines is about 150 kHz. The measurements were mainly done with $\vec{H}$ in a (110) plane when several Ga neighbors are equivalent (see Fig. 1) resulting in seven distinct ENDOR lines. Then a total number of 252 Ga ENDOR lines is expected, which is in agreement with the observations.

The assignment of a number of lines in the spectrum to ^{69}Ga and ^{71}Ga was done by use of Eqs. (2) and (3). First, we looked for pairs of ENDOR lines whose ratios of transition frequencies correspond approximately to $^{69}\gamma/^{71}\gamma = 0.7870$.[14] These lines are ascribed to the central ENDOR transitions $|M, +\frac{1}{2}\rangle \rightarrow |M, -\frac{1}{2}\rangle$. Second, the characteristic Zeeman shifts were observed. Third, an accurate use of Eq. (2) with $\vec{H}$ along x_h enabled us to predict the separations of the central transitions belonging to $M = \pm\frac{5}{2}$ for each Ga isotope, using the Ga NMR frequencies.[14]

In the spectrum only some regions were found where the complete angular dependence of ENDOR transitions could be followed. One such region is the upper part of the spectrum where the angular diagram shown in Fig. 2 was made. The lines are assigned to ^{71}Ga for one of the multiplets $M = \pm\frac{5}{2}$ (in Sec. III D *1* we arrive at $M = -\frac{5}{2}$). For convenience the figure is split into three parts each corresponding to a particular $m \rightarrow m-1$ transition (further denoted by n, where $n = m - \frac{1}{2}$). The symmetry properties of the angular diagrams do not enable us to assign the Ga ENDOR lines to a specific shell. However, the characteristic patterns of Fig. 2 restrict the possibilities to shells contained in the {110} plane symmetry class[15]; i.e., Mn and Ga both lie in {110} planes. It is most likely, and we have assumed this earlier, that the lines belong to the shell of Ga atoms on next-nearest-neighbor sites. The assignment of the curves of Fig. 2 to specific Ga neighbors is represented by letter symbols, corresponding to those in the unit cell of Fig. 1.

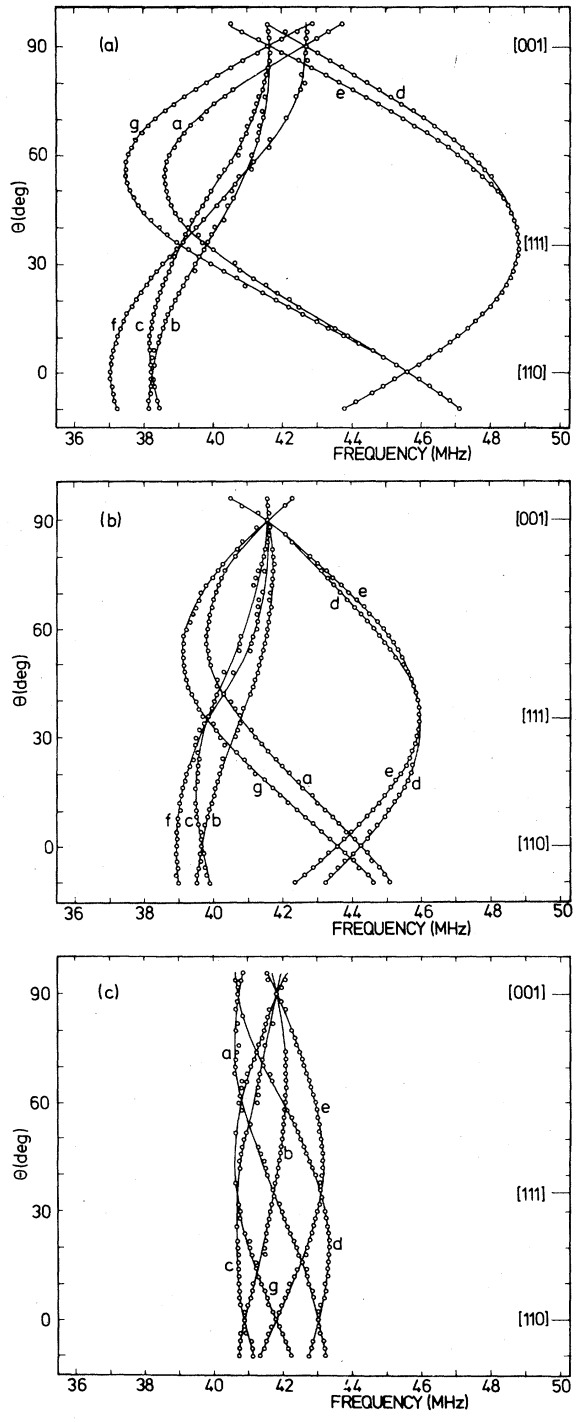

FIG. 2. Measured angular diagrams of ENDOR transitions in the upper part of the Ga ENDOR spectrum with $\vec{H}$ in the $(\bar{1}10)$ plane. θ is the angle between $\vec{H}$ and [110]. $H = 3244.5$ G. The transitions are assigned to the 12 nearest ^{71}Ga neighbors for $M = -\frac{5}{2}$. The $n = +1$, 0, and -1 Ga spin transitions are presented separately in (a), (b), and (c), respectively. The letters a to g near the curves refer to the Ga neighbors labeled in Fig. 1.

The curves d of Fig. 2 reflect the directional properties of the interactions within the Ga_d-Mn pair. The angular position at which curve d with $n = 0$ has a maximum frequency corresponds to the principal axis x_h: the angle α defined in Fig. 1 is $32.0 \pm 0.5°$. At each angle the three curves d are found to be approximately equidistant, which is in accordance with the third term of Eq. (2). The angular position at which the separation is largest corresponds to the principal axis x_q: the angle β of Fig. 1 is found to be $43 \pm 1°$. Further, we note that α and β have the same sign.

In our description of the spectrum the three curves d of Fig. 2 were assigned to Ga_d. It is easily seen that experimentally these curves may also be attributed to Ga_a. The reason why we favor Ga_d is that, at first sight, it provides a more adequate physical model in which x_h points approximately along the line from Ga_d to the P atom which is bonded to both the Ga_d and Mn ions, as in Fig. 1 with $\alpha > 0$. This tentative assignment has no effect on the values of the interactions. We will return to this point in Sec. IV A.

There are some other regions of the ENDOR spectrum where in more or less detail the angular dependence of a part of the spectrum could be followed. These are presented in Figs. 3 and 4. The assignments, given in the figures, are consistent with assignment of the upper part of the spectrum (Fig. 2) to $M = -\frac{5}{2}$.

D. Determination of parameters

1. Sign of A

The curves of Fig. 2 were tentatively assigned to $M = -\frac{5}{2}$, and consequently the hyperfine field $A/g_N\beta_N$ is positive. Since $g_N > 0$, A therefore is positive. The assignment to $M = -\frac{5}{2}$ is based on a comparison of ENDOR results obtained for the trigonal Mn^{2+} center with those for the cubic center. For a trigonal center one can unambiguously assign an ENDOR line to a state $|M\rangle$ because the EPR fine-structure transitions do not overlap. We actually measured ENDOR spectra with $\vec{H} \parallel [111]$, and fixed at the EPR transitions $\pm\frac{5}{2} \rightarrow \pm\frac{3}{2}$, both in one center with trigonal axis along [111]. The ENDOR line with the highest frequency was found at approximately 39 MHz for ENDOR within $|-\frac{5}{2}\rangle$, and 30 MHz within $|+\frac{5}{2}\rangle$. Because we do not expect marked differences between cubic and trigonal Mn^{2+} centers concerning the hfi with next nearest neighbors, the lines in the upper part of the ENDOR spectrum, Fig. 2, are assigned to $M = -\frac{5}{2}$.

2. Hyperfine constants

For the analytical determination of the A_{ii}'s with the help of Eqs. (2) and (3) we used the frequencies

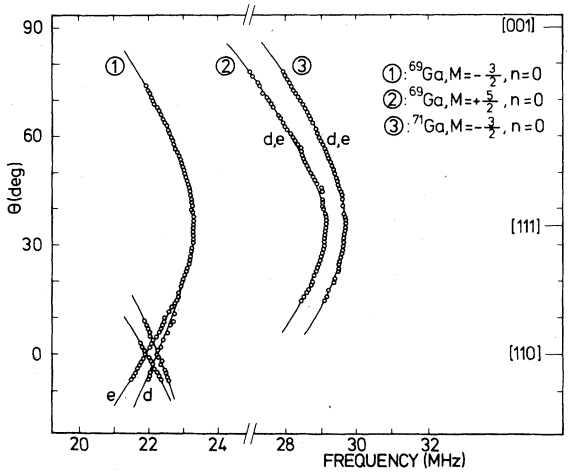

FIG. 3. Measured angular diagrams near 23 and 29 MHz with $\vec{H}$ in the $(\bar{1}10)$ plane. $H = 3530.4$ G.

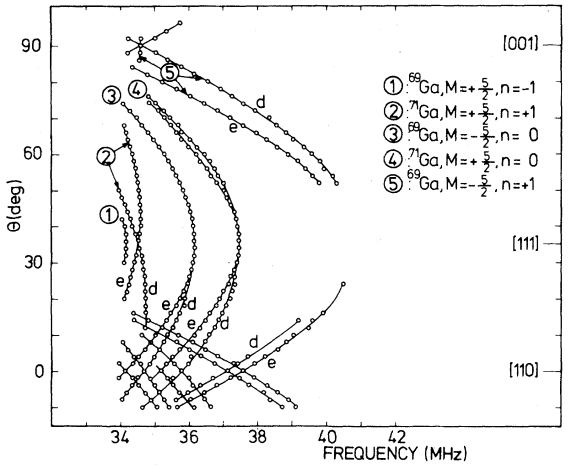

FIG. 4. Measured angular diagram near 36 MHz with $\vec{H}$ in the $(\bar{1}10)$ plane. $H = 3244.5$ G.

of the $n = 0$ lines d, a, and f of Fig. 2(b) with $\vec{H}$ parallel to $x_h(d)$, $y_h(a)$, and $z_h(f)$. A check on $A_{x_h x_h}$ was provided by the maxima of the $n = 0$ curves d in Figs. 3 and 4.

The QI parameters Q' (including its sign) and η were determined by measuring the separations of several $n = \pm 1$ to 0 lines when $\vec{H}$ is parallel to x_h, y_h, and z_h. If we omit the second-order contributions due to QI (~ 10 kHz), Eq. (2) shows that the $n = 1$, 0, and -1 lines are equidistant. The separation, with $\vec{H}$ along a principal axis i of the hfi tensor, is

$$Q'(3\cos^2\varphi - 1 + \eta\sin^2\varphi) - \frac{M(A_{jj}^2 + A_{kk}^2)}{2g\beta H}, \quad (4)$$

and thus depends on M and φ (insert $\varphi = \frac{1}{2}\pi$ and $\eta = -\eta$ for $i = z_h$). It was found that the separation of the lines d of Fig. 2, corresponding to $\{^{71}\text{Ga}, M = -\frac{5}{2}\}$, is slightly smaller than that of $\{^{71}\text{Ga}, M = +\frac{5}{2}\}$ when $\vec{H} \| x_h$. Then Eq. (4) predicts Q'/M to be positive for the curves d of Fig. 2. Since $MA < 0$ for these curves, we have $Q'/A < 0$. For A positive we then obtain $Q' < 0$. An independent check on the negative sign of Q'/A was made by comparing the separations of the $n = \pm 1$ lines to the $n = 0$ line of $\{^{71}\text{Ga}, M = -\frac{5}{2}\}$ along $x_h(\varphi = 11°)$, $y_h(\varphi = 101°)$, and $z_h(\varphi = \frac{1}{2}\pi, \eta = -\eta)$ using Eq. (4). The first term of Eq. (4) changes sign, whereas the second term is virtually constant. Further, the separation of the $n = -1$ to 0 line of $\{^{69}\text{Ga}, M = +\frac{5}{2}\}$ when $\vec{H} \| x_h$ could be predicted from the results of ^{71}Ga, using the ratio of the nuclear quadrupole moments $^{69}Q/^{71}Q = 1.587$.[14]

The analytically determined parameters, listed in Table I, were used as starting values for computer calculations using matrix diagonalization. As we

TABLE I. Experimental ^{71}Ga hfi parameters at 4.2 K as determined by perturbation methods and computer diagonalization.

		Perturbation theory	Diagonalization
$A_{x_h x_h}$	(MHz)	+16.66	+16.665 ± 0.004
$A_{y_h y_h}$	(MHz)	+14.19	+14.186 ± 0.010
$A_{z_h z_h}$	(MHz)	+13.85	+13.848 ± 0.008
A_s	(MHz)	+14.90	+14.900 ± 0.007
$\lvert\alpha\rvert$[a]	(degrees)	32.0	32.2 ± 0.2
Q'	(MHz)	−1.50	−1.493 ± 0.005
η		0.19	0.20 ± 0.02
$\lvert\beta\rvert$[a]	(degrees)	43.0	42.6 ± 0.3
$g_N\beta_N$	(kHz/G)	+1.298	+1.298 ± 0.003

[a]The signs of α and β are the same.

have seen, the splittings of the energy levels belonging to the states $|M,m_{\mathrm{Mn}},m_{\mathrm{Ga}}\rangle = |+\frac{5}{2},+\frac{5}{2},m_{\mathrm{Ga}}\rangle$ and $|-\frac{5}{2},-\frac{5}{2},m_{\mathrm{Ga}}\rangle$ are correctly described within the set of 24 basic states $|M,m_{\mathrm{Ga}}\rangle$, so we used the diagonalization of a 24×24 matrix. The diagonalization was done for about 40 experimental frequencies. With the set of ^{71}Ga hfi parameters listed in the last column of Table I, a best fit to the experimental frequencies (within the experimental errors of 10–30 kHz) was obtained. It is noted that there is a remarkable closeness of the results from perturbation theory and diagonalization. The results for ^{69}Ga were found to scale with those for ^{71}Ga according to the ratios of the nuclear spins and the quadrupole moments.[14]

IV. ORIGINS OF THE HYPERFINE INTERACTIONS

It is the aim of this section to gain some insight into the possible origins of the hfi's. In general, this is quite a complicated subject because there are many contributions to the interactions. We must therefore make it clear that we do not intend to give a detailed theory, but merely discuss a simple model which partly explains the data. We shall first comment on the magnetic hfi, and subsequently discuss the origins of the QI.

A. Magnetic hfi

As can be seen from Table I, the hfi is mainly isotropic. Its value A_s for ^{71}Ga is included in this table. Following Huang *et al.*[16] we assume that the isotropic hfi is mainly caused by transfer of Mn $3d$ up spins to the first empty s shell of the cation, i.e., the Ga $4s$ shell. A fraction f_s of unpaired spin in a Ga s orbit gives rise to an isotropic hfi $A_s = f_s A_s^0/2S$ in which $A_s^0 = \frac{16}{3}\pi\beta g_N\beta_N|\psi(0)|^2$. Using the tables of SCF (self-consistent-field) orbitals of Clementi,[17] we find by extrapolation from Ga^0 over Ga^+ to $Ga^{2+}(3d^{10}4s)$ a value of 12.0 GHz for $^{71}A_{4s}^0/h$. This figure will be reduced by covalency: for Ga^{2+} substituted in ZnS an experimental value of 7.7 GHz has been determined.[18] If we insert the latter figure we find $f_{4s} = +0.010$ which is a reasonable value.

The anisotropic contribution A_{aniso} consists of two parts: the dipolar interaction between the Mn electronic spin and the Ga nuclear spin, and the interaction due to unpaired Ga p electrons. The experimental $\vec{\mathrm{A}}_{\mathrm{aniso}}^{\mathrm{expt}}$ is presented in Table II. This table will be used for a further analysis of the hfi's. Assuming point dipoles, the dipolar interaction tensor A_{dd} was calculated with the Ga-Mn distance taken from the undeformed GaP lattice; i.e., $r = 3.85$ Å. We subtract $\vec{\mathrm{A}}_{dd}$ from $\vec{\mathrm{A}}_{\mathrm{aniso}}^{\mathrm{expt}}$ and find a new tensor $A(p)$[19] which describes the effect of occupation of non-s orbitals of Ga caused by overlap and transfer of electron spin. $\vec{\mathrm{A}}_{dd}$ and $\vec{\mathrm{A}}(p)$ are included in Table II. The angle α' defining the position of $\vec{\mathrm{A}}(p)$ is found to have the same sign as α.

We assume next that the most important process leading to $\vec{\mathrm{A}}(p)$ is the indirect transfer of $3d$ electrons to the empty Ga $4p$ orbitals via the intervening P ligand. Such an indirect process is probably predominant in a covalent crystal. It is interesting to find the differences of the spin densities in the Ga $4p$ orbitals. The axes of the $4p$ orbitals are taken to be the same as the principal axes of $\vec{\mathrm{A}}(p)$. On this basis one can write

$$\vec{\mathrm{A}}(p) = \frac{A_{4p}}{2S}\begin{pmatrix} 2f_x - f_y - f_z & & \\ & 2f_y - f_z - f_x & \\ & & 2f_z - f_x - f_y \end{pmatrix}, \tag{5}$$

TABLE II. Experimental hfi tensors of ^{71}Ga and calculated contributions. The A and B tensors are related to anisotropic magnetic hfi and QI, respectively. The tensors are given in the diagonal form. The position of each principal x axis is presented in the last column. The signs of α, β, and α' are the same. The positive sign is consistent with the model described in Sec. IV A.

	Diagonal tensor elements (MHz)			Angle between x axis and [110] (degrees)	
	xx	yy	zz		
$A_{\mathrm{aniso}}^{\mathrm{expt}}$	+1.76	−0.71	−1.05	$\lvert\alpha\rvert =$	32.2
A_{dd}	+0.84	−0.42	−0.42		0
$A(p)$	+1.44	−0.81	−0.63	$\lvert\alpha'\rvert =$	47.4
B^{expt}	−1.00	+0.40	+0.60	$\lvert\beta\rvert =$	42.6
$B(p)$	−0.21	+0.12	+0.09	$\lvert\alpha'\rvert =$	47.4
B_{Mn}	−0.24	+0.12	+0.12		0
B_{P}	−0.12	+0.09	+0.03		+69.2

where $A_{4p}=\frac{4}{5}\beta g_N\beta_N\langle r^{-3}\rangle_{4p}$. Substitution of $\langle r^{-3}\rangle_{4p}=2.891$ a.u.[20] yields $f_x-f_y=+0.020$ and $f_x-f_z=+0.018$. The indirect transfer process should result in an axial hfi tensor with unique axis pointing along the line from Ga to the intervening P. Consequently, α' is expected to be approximately $+35.3°$ (see Fig. 1). Moreover the up-spin transfer predicts $f_\sigma-f_\pi>0$. Now, $\vec{\mathrm{A}}(p)$ indeed shows a nearly uniaxial interaction (see Table II) with the correct sign for the differences of spin densities. The deviation of α' in Table II from the expected $+35.3°$ is smallest if we take $\alpha'=+47.4°$. Since the angles α', α, and β were found to have the same sign, α and β are also positive. Therefore the experimental x_h and x_q axes are positioned as shown in the lower part of Fig. 1.

B. Quadrupole interaction

It is convenient at this point to express the QI in tensor form. We take the QI Hamiltonian as $\vec{\mathrm{I}}\cdot\vec{\mathrm{B}}\cdot\vec{\mathrm{I}}$ and find the experimental tensor B^{expt} which is listed in Table II. This table shows that the angles α' and β are nearly the same, which suggests that the QI might have as its main source the field gradient built up by the electron cloud of Ga. In those cases where transfer of electrons with definite spin direction occurs, as we assumed, charge and spin distributions are the same so that the contribution to the QI can be calculated from $\vec{\mathrm{A}}(p)$. This contribution will be designated $\vec{\mathrm{B}}(p)$. Using Ref. 21, the relationship between the components of $\vec{\mathrm{B}}(p)$ and $\vec{\mathrm{A}}(p)$ is found to be

$$\frac{B_{ii}(p)}{A_{ii}(p)}=-\frac{Se^2Q(1-R)}{2I(2I-1)\beta g_N\beta_N} \tag{6}$$

for the case of transfer to an empty p shell. Q is the quadrupole moment and R is the atomic (anti) shielding factor. With $Q(1-R)=+0.120\times10^{-24}$ cm^2 for ^{71}Ga,[14] we find $B_{ii}(p)/A_{ii}(p)=-0.145$. Table II contains the calculated $\vec{\mathrm{B}}(p)$ which is seen to be only $\sim20\%$ of the experimental QI.

We will now give a rough estimate of two contributions to the field gradient due to external charges which stem from the mismatch of Mn^{2+} at a Ga^{3+} site. There is mismatch of charge (Mn_-) and of ionic radius. The latter causes deformation of the lattice around the Mn^{2+} ion. The field gradients were computed using the point-charge approximation. The ionic Sternheimer[20] antishielding factor $1-\gamma_\infty=10.8$ is taken into account. The contribution due to Mn_- was calculated with the Ga-Mn distance as present in the undeformed crystal, and neglecting the contribution from the polarization of the crystal.[22] The resultant B_{Mn_-} tensor is listed in Table II. The second contribution is caused by the lattice deformation whose size may be estimated by comparing the radii of Mn^{2+} and Ga^{3+}: the ionic radii are 0.80 and 0.62 Å,[23] while the covalent radii are 1.299 and 1.225 Å,[24] respectively. It is therefore reasonable to suppose that the neighboring atoms are pushed away. A good estimate of the deformation induced field gradients at the Ga ion is obtained by considering only the shift (in the $[\bar{1}\bar{1}1]$ direction) of the P ion which is bonded to both the Mn^{2+} ion and the Ga ion (see Fig. 1, lower part). We assume an increase of the Mn-P distance with 0.15 Å, and effective ionic charges of -1 on the P ions.[25] Then we find the B_{P_-} tensor given in Table II. We learn from this table that the point-charge contributions account for about 30% of the observed $\vec{\mathrm{B}}^{\mathrm{expt}}$, but with different directions of the principal axes.

Other mechanisms, whose contributions are even more difficult to estimate, are overlap distortion of the Ga closed-shell orbitals by the surrounding P ligands,[26,27] and covalent transfer from P to Ga $4p$ orbitals. Both mechanisms may play a role because the orbitals of the intervening P ion are modified by the presence of the Mn^{2+} ion. The effects are further complicated by the deformation of the lattice.

V. CONCLUSIONS

ENDOR spectra comprising some 200 lines below 50 MHz have been observed for the cubic Mn^{2+} center. The observed lines can be ascribed to the shell of 12 nearest Ga neighbors. The magnetic hfi and electric QI tensors have been determined. The spectra are quite complex because the principal axes of the tensors do not coincide. The magnetic hfi is found to be mainly isotropic. A comparison with Ga ENDOR transitions belonging to a trigonal Mn^{2+} center allows us to assign quantum numbers to the ENDOR transitions and to conclude that the hyperfine field is positive.

An attempt was made to interpret the data using a simple model. One mechanism which contributes to the magnetic hfi as well as to the QI is the transfer of Mn $3d$ electrons to empty Ga $4s$ and $4p$ orbitals. Reasonable spin transfer coefficients are found on this basis. The assumption that the transfer to $4p$ orbitals is indirect, via the intervening P ligand, provides an explanation for the nondipolar anisotropic magnetic hfi, and removes the ambiguity about the assignment of a specific hfi tensor to a specific Ga site of the shell. Two other contributions to the QI, due to external charges, are induced by the mismatch of the Mn^{2+} ion at a Ga^{3+} site. The combined contributions account for about half of the experimental QI.

ACKNOWLEDGMENTS

I would like to thank A. T. Vink and H. J. A. van Dijk for providing the single crystals, R. P. van Stapele, P. R. Locher, B. S. Blaisse, and D. van Ormondt for helpful discussions, and R. C. Peters, A. T. Vink, and H. Mulder for performing Hall-effect measurements.

[1]E. Šimánek and Z. Šroubek, in *Electron Paramagnetic Resonance,* edited by S. Geschwind (Plenum, New York, 1972).
[2]D. R. Taylor, J. Owen, and B. M. Wanklyn, J. Phys. C 6, 2592 (1973).
[3]T. L. Estle and W. C. Holton, Phys. Rev. 150, 159 (1966).
[4]G. W. Ludwig and M. R. Lorenz, Phys. Rev. 131, 601 (1963). We note that in this paper the four ENDOR lines reported near 21 MHz are incorrectly assigned to $M=-\frac{3}{2}$, which yields hyperfine parameters being at variance with the EPR spectrum. An assignment to $M=\pm\frac{1}{2}$, giving $|A_{Cd}/h|\sim 31.9$ MHz, removes the discrepancy.
[5]W. Teuerle, E. Blaschke, and A. Hausmann, Z. Phys. 270, 37 (1974); W. Teuerle and A. Hausmann, Z. Phys. B 23, 11 (1976).
[6]P. van Engelen, in *Proceedings of the Eighteenth Ampère Congress, Nottingham, 1974,* edited by P. S. Allen, E. R. Andrew, and C. A. Bates (North-Holland, Amsterdam, 1975), p. 445.
[7]R. S. Title and T. S. Plaskett, Appl. Phys. Lett. 14, 76 (1969).
[8]A. T. Vink (private communication).
[9]The CdTe:Cr^+ system of Ref. 4 is very similar to ours; both centers are compensated acceptors in the $3d^5$ configuration, and the host lattices are both zinc blende.
[10]G. G. P. van Gorkom and A. T. Vink, Solid State Commun. 11, 767 (1972).
[11]H. H. Woodbury and G. W. Ludwig, Bull. Am. Phys. Soc. 6, 118 (1961).
[12]P. van Engelen and S. G. Sie, Solid State Commun. 30, 515 (1979).
[13]L. C. Kravitz and W. W. Piper, Phys. Rev. 146, 322 (1966); R. K. Jeck and J. J. Krebs, Phys. Rev. B 5, 1677 (1972).
[14]G. H. Fuller and V. W. Cohen, Nucl. Data Tables A 5, 433 (1969).
[15]E. B. Hale and R. L. Mieher, Phys. Rev. 184, 739 (1969).
[16]Nai Li Huang, R. Orbach, and E. Šimánek, Phys. Rev. Lett. 17, 134 (1966); Nai Li Huang, R. Orbach, E. Šimánek, J. Owen, and D. R. Taylor, Phys. Rev. 156, 383 (1967).
[17]E. Clementi, IBM J. Res. Dev. 9, 2 (1965).
[18]A. Räuber and J. Schneider, Phys. Status Solidi 18, 125 (1966).
[19]In Ref. 6 the figures for this tensor are in error.
[20]R. M. Sternheimer, Phys. Rev. A 6, 1702 (1972).
[21]J. Owen and J. H. M. Thornley, Rep. Prog. Phys. 29, 675 (1966).
[22]M. H. Cohen and F. Reif, in *Solid State Physics,* edited by F. Seitz and D. Turnbull (Academic, New York, 1957), Vol. 5.
[23]L. H. Ahrens, Geochim. Cosmochim. Acta 2, 155 (1952).
[24]J. A. van Vechten and J. C. Phillips, Phys. Rev. B 2, 2160 (1970).
[25]W. A. Harrison and S. Ciraci, Phys. Rev. B 10, 1516 (1974).
[26]D. R. Taylor, J. Chem. Phys. 48, 536 (1968).
[27]G. A. Sawatzky, F. van der Woude, and J. Hupkes, J. Phys. (Paris) 32, C1-276 (1971); R. R. Sharma, Phys. Rev. Lett. 25, 1622 (1970).